

Biomass waste-assisted micro(nano)plastics capture, utilization, and storage for sustainable water remediation

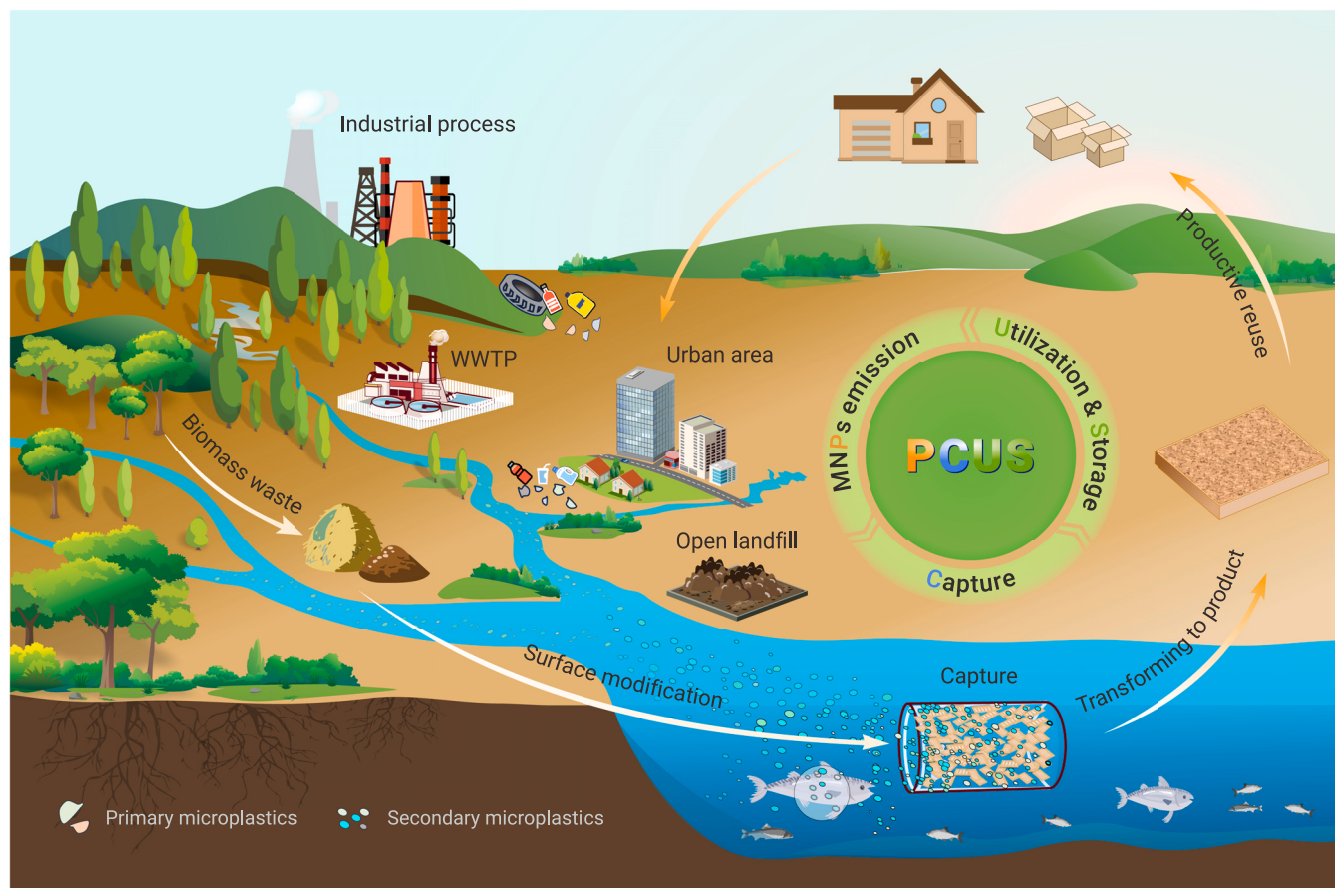
Lu Chen,^{1,5} Tingting Bi,^{1,5} Erlantz Lizundia,^{2,3} Anxiong Liu,^{1,4} Luhe Qi,¹ Yifan Ma,¹ Jing Huang,¹ Ziyang Lu,¹ Le Yu,¹ Hongbing Deng,^{1,*} and Chaoji Chen^{1,*}

*Correspondence: hbdeng@whu.edu.cn (H.D.); chenchaojili@whu.edu.cn (C.C.)

Received: February 3, 2024; Accepted: June 3, 2024; Published Online: June 7, 2024; <https://doi.org/10.1016/j.xinn.2024.100655>

© 2024 The Authors. Published by Elsevier Inc. on behalf of Youth Innovation Co., Ltd. This is an open access article under the CC BY-NC-ND license (<http://creativecommons.org/licenses/by-nc-nd/4.0/>).

GRAPHICAL ABSTRACT



PUBLIC SUMMARY

- Micro(nano)plastic capture, utilization, and storage (PCUS) strategy is proposed for the first time to mitigate plastic pollution.
- Excellent capture performance toward various micro(nano)plastics has been demonstrated under complex water conditions.
- The effective removal is driven by multiscale interactions and cluster-like aggregate sedimentation.
- Low-carbon-footprint PCUS strategy presents environmental sustainability and economic feasibility.



Biomass waste-assisted micro(nano)plastics capture, utilization, and storage for sustainable water remediation

Lu Chen,^{1,5} Tingting Bi,^{1,5} Erlantz Lizundia,^{2,3} Anxiong Liu,^{1,4} Luhe Qi,¹ Yifan Ma,¹ Jing Huang,¹ Ziyang Lu,¹ Le Yu,¹ Hongbing Deng,^{1,*} and Chaoji Chen^{1,*}

¹Hubei Biomass-Resource Chemistry and Environmental Biotechnology Key Laboratory, School of Resource and Environmental Sciences, Wuhan University, Wuhan 430079, China

²Life Cycle Thinking Group, Department of Graphic Design and Engineering Projects, University of the Basque Country (UPV/EHU), 48013 Bilbao, Spain

³BCMaterials, Basque Center for Materials, Applications and Nanostructures, Edif. Martina Casiano, 48940 Leioa, Spain

⁴Zhongnan Hospital of Wuhan University, Wuhan University, Wuhan 430071, China

⁵These authors contributed equally

*Correspondence: hbdeng@whu.edu.cn (H.D.); chenchaojili@whu.edu.cn (C.C.)

Received: February 3, 2024; Accepted: June 3, 2024; Published Online: June 7, 2024; <https://doi.org/10.1016/j.xinn.2024.100655>

© 2024 The Authors. Published by Elsevier Inc. on behalf of Youth Innovation Co., Ltd. This is an open access article under the CC BY-NC-ND license (<http://creativecommons.org/licenses/by-nc-nd/4.0/>).

Citation: Chen L., Bi T., Lizundia E., et al., (2024). Biomass waste-assisted micro(nano)plastics capture, utilization, and storage for sustainable water remediation. *The Innovation* 5(4), 100655.

Micro(nano)plastics (MNPs) have become a significant environmental concern due to their widespread presence in the biosphere and potential harm to ecosystems and human health. Here, we propose for the first time a MNPs capture, utilization, and storage (PCUS) concept to achieve MNPs remediation from water while meeting economically productive upcycling and environmentally sustainable plastic waste management. A highly efficient capturing material derived from surface-modified woody biomass waste (M-Basswood) is developed to remove a broad spectrum of multidimensional and compositional MNPs from water. The M-Basswood delivered a high and stable capture efficiency of >99.1% at different pH or salinity levels. This exceptional capture performance is driven by multiscale interactions between M-Basswood and MNPs, involving physical trapping, strong electrostatic attractions, and triggered MNPs cluster-like aggregation sedimentation. Additionally, the *in vivo* biodistribution of MNPs shows low ingestion and accumulation of MNPs in the mice organs. After MNPs remediation from water, the M-Basswood, together with captured MNPs, is further processed into a high-performance composite board product where MNPs serve as the glue for utilization and storage. Furthermore, the life cycle assessment (LCA) and techno-economic analysis (TEA) results demonstrate the environmental friendliness and economic viability of our proposed full-chain PCUS strategy, promising to drive positive change in plastic pollution and foster a circular economy.

INTRODUCTION

Rapidly rising levels of plastic pollution represent a serious global environmental problem, negatively impacting ecological, social, economic, and health aspects of sustainable development.^{1–3} According to the United Nations Environment Programme, under a business-as-usual scenario and in the absence of necessary interventions, the amount of plastic waste entering aquatic ecosystems could nearly triple from 9–14 million tons per year in 2016 to a projected 23–37 million tons per year by 2040.⁴ Up to 12 million tons of plastics find their way into the oceans each year, now making up 80% of all marine pollutions.⁵ These plastics can erode into potentially toxic micro(nano)plastics (MNPs) through natural weathering that are found in the global food chain and even the human body.^{6–8} Omnipresent MNPs are tiny plastic particles often less than 5 mm in size, which can seep through filtration and treatment facilities and end up in our food and waterways, thereby posing a big and growing threat to global ecosystems and human health as a consequence of its poor reversibility and ubiquitous global accumulation.^{9,10} Facing this global emergency that goes beyond national borders, the Global Plastics Treaty in progress rightly urges nations to reduce plastic pollution across the full life cycle,¹¹ including MNPs pollution in the ocean, especially covering plastic waste management, plastic pollution mitigation, and opportunities for reduction, redesign, and reuse toward a circular economy.

Recently, in the collective effort to fight decarbonization and net-zero ambitions with a worldwide 7 gigatonnes per annum (Gtpa) target to be reached by 2050,^{12–14} CCUS (carbon capture, utilization, and storage) is emerging as an indispensable and multifaceted approach to managing carbon emissions.^{15–18} In particular, CCUS technology involves the capture of CO₂, generally from large point sources like power generation or industrial facilities. If not being used on site, then the captured CO₂ is compressed, transported, and utilized in a range

of applications or injected into deep geological formations for permanent storage. According to the latest market research study published by Zion Market Research,¹⁹ the demand analysis of CCUS technologies market size and share revenue was valued at around USD 2,500 million in 2022 and is estimated to increase to USD 7,900 million by 2030, at a compound annual growth rate of approximately 15.5%. Given the collaboration and lessons from existing economically viable and practical CCUS technology for climate change, here, an innovative modular concept of MNPs capture, utilization, and storage (PCUS) is first proposed to mitigate plastic pollution, aiming at achieving environmental remediation of MNPs from water, economically productive use of MNPs, and environmentally sustainable plastic waste management (Figure 1A). PCUS plays a different role from single MNPs removal in long-term and net-zero plans developed by many countries for reducing plastic emissions. Promisingly, the global MNPs crisis brings about both challenges and opportunities, which inspires us to think about the profound rewards for a sustainable society if we can unlock the potential of MNPs to make them useful while keeping them out of the water.

In this work, natural biomass waste (e.g., wood, straw, and bamboo) is used to demonstrate the full-chain PCUS concept we proposed for plastic pollution (Figures 1A and 1B). According to the US Environmental Protection Agency, the global capacities for wood waste and plastics are notable (Figure 1C),²⁰ which opens up possibilities for an integrated PCUS strategy using woody biomass waste. Benefiting from wood's inherent physical robustness and chemical structure with abundant functional groups as a result of its multicomponent nature, which includes cellulose, hemicellulose, and lignin, this material can be facilely surface engineered for efficient capture of MNPs from water (Figures S1 and S2). This surface-modified wood waste (M-Basswood) exhibited an excellent capture performance of MNPs with different dimensions and chemical compositions, and its performance can remain stable at different pH and salinity levels, suggesting its potential for MNPs removal from practical wastewater. This high performance was driven by multiscale interactions, involving the physical trapping, strong electrostatic attraction, hydrogen bonding, and π - π stacking between M-Basswood and MNPs, as well as triggered MNPs cluster-like self-aggregating sedimentation (Figure 1A), which provides a facile and efficient way for separating MNPs from water. Apart from the environmental benefits of water remediation, M-Basswood, together with captured MNPs, can be directly processed into a formaldehyde-free composite (wood-plastic) board where MNPs serve as a strong glue for further utilization and storage (Figure 1A). Attractively, this composite board demonstrated low environmental impacts and economic competitiveness throughout the full-chain PCUS process. This environmentally sustainable, low-carbon-footprint, economically viable PCUS strategy with waste recycling opens an integral pathway for mitigating plastic pollution and fostering a circular economy, thereby contributing greatly toward sustainability.

RESULTS AND DISCUSSION

Structural and chemical characterizations of M-Basswood

As a proof-of-concept demonstration, natural basswood waste was initially used to illustrate the PCUS concept for MNPs remediation (Figure 2A). Basswood cells displayed a hierarchical porous microstructure composed of an interconnected network of cellulose, hemicelluloses, and lignins (Figures 2B and S3).^{21–23} Such a feature was beneficial for the

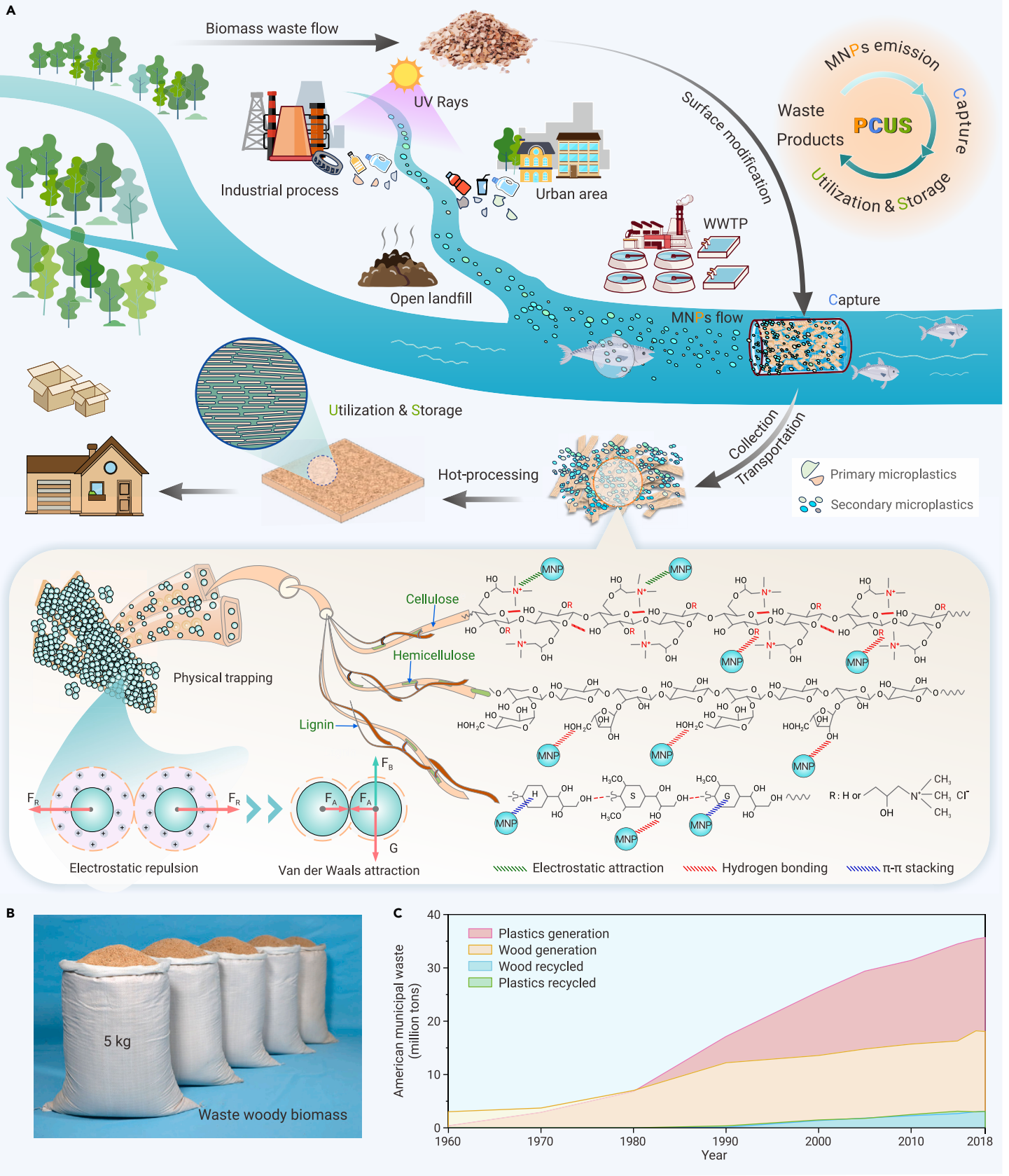


Figure 1. Schematic illustration of biomass-based PCUS for water remediation (A) Resource-abundant surface-engineered biomass waste (e.g., wood, straw, and bamboo) is used for MNPs removal from water ecosystems via multiscale interactions between M-Basswood and MNPs, as well as triggered self-aggregation sedimentation, followed by economically productive reuse of these MNPs based on the full-chain MNPs capture, utilization, and storage (PCUS) strategy. (B) Photograph showing woody biomass waste. (C) Amount of plastic and wood waste generation based on statistics from 1960 to 2018 provided by the US Environmental Protection Agency.

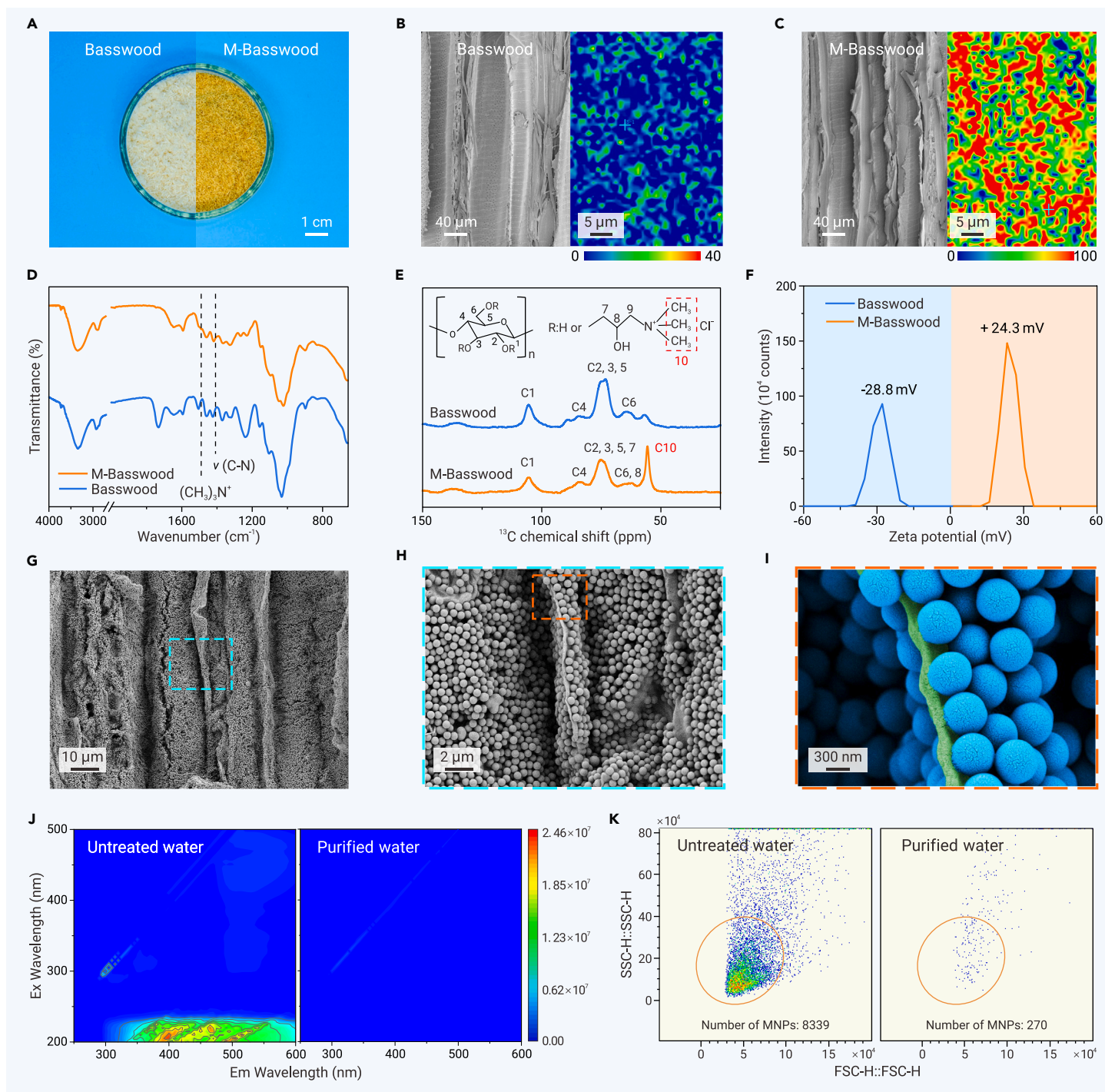


Figure 2. Structural and chemical characterizations of M-Basswood (A) Photograph showing the natural basswood and the surface-functionalized M-Basswood. (B and C) SEM and 2D Raman images of natural basswood (B) and M-Basswood (C). (D) FTIR analysis of basswood and M-Basswood. (E) ^{13}C solid-state magic angle spinning (MAS) NMR spectra of the basswood and M-Basswood. (F) Zeta potentials of basswood and M-Basswood. (G–I) SEM images of M-Basswood after the capture of PS particles. (J and K) Three-dimensional excitation-emission matrix (3D-EEM) fluorescence spectra (J) and the number of PS particles determined by flow cytometry (K) before and after M-Basswood treatment.

surface functionalization of basswood waste via etherification treatment by 3-chloro-2-hydroxypropyltrimethylammonium chloride (CHPTAC), a widely non-toxic etherifying agent for the cationization reaction.²⁴ Upon chemical modification, the initially light yellow wood turned a yellow-brownish color. The M-Basswood with an initial porous structure presented a smooth and hydrophilic surface, which enhances its functionalities in the water purification process (Figures 2C, S3, and S4). Additionally, from the two-dimensional (2D) Raman spectrum of the M-Basswood, where the red regions represent the grafting and blue represent the opposite, the CHPTAC-grafted regions evenly distributed on M-Basswood increased and exhibited a much larger peak intensity at 761 cm^{-1} , assigned to the characteristic band of

CHPTAC (Figures 2C and S5),²⁵ revealing the homogeneous surface modification of the M-Basswood.

To confirm the chemical composition of the as-prepared M-Basswood, Fourier transform infrared (FTIR) and ^{13}C nuclear magnetic resonance (NMR) combined with X-ray photoelectron spectroscopy (XPS) analysis were performed. Compared to natural basswood, two absorption bands at $1,489$ and $1,419\text{ cm}^{-1}$ of M-Basswood corresponding to the trimethyl groups of the quaternary ammonium and C–N stretch emerge,²⁶ respectively, validating the successful incorporation of CHPTAC (Figure 2D). Complementary to FTIR, ^{13}C NMR further provides detailed information about the variation of molecular-level interactions in the investigated M-Basswood. As presented in Figure 2E, the ^{13}C NMR

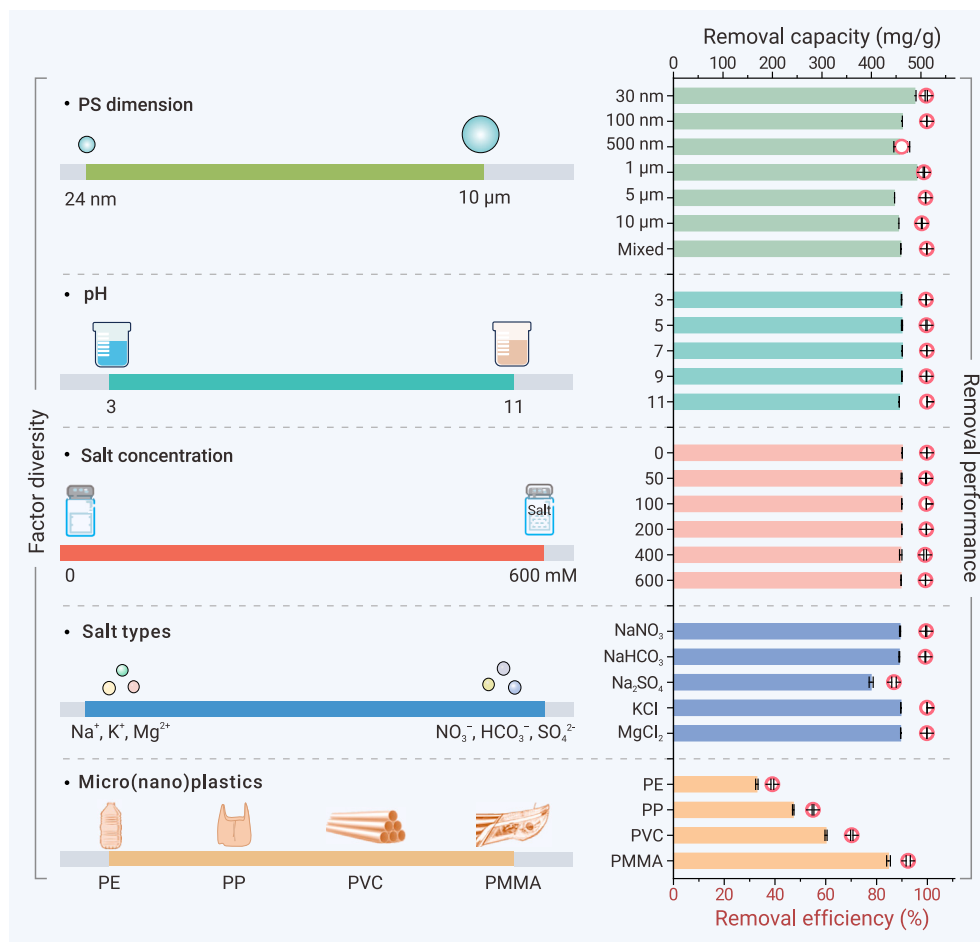


Figure 3. MNPs capture performance of M-Basswood Left, schematic representation of the dimensions, pH, salt presence (concentration and types), and species of MNPs investigated in this work. Right, the removal performance of MNPs in various water systems. The MNPs used in this work cover PMMA (spheres, negatively charged, 100 nm), PP (spheres, negatively charged, 500 nm), PVC (spheres, negatively charged, 1 μm), and PE (spheres, negatively charged, 500 nm). The concentration of these MNPs was 1 mg/mL. $n = 3$, error bar represents the standard error of the mean.

collaboratively confirm the excellent MNPs capturing capability of M-Basswood from water.

MNPs capture performance of M-Basswood

As an omnipresent emerging group of contaminants, MNPs feature multidimensional diversity, a different chemical nature, and a recalcitrant character. To offer a broad-spectrum investigation of the MNPs capture performance by M-Basswood, we carried out a series of MNPs remediation experiments under various pertinent scenarios (Figure 3). We first demonstrated the capture capability of M-Basswood using spherical PS MNPs, and their size distributions and zeta potentials are provided in Figures S8 and S9. Initially stable and well dispersed in water, the PS particles were efficiently captured after M-Basswood treatment, with cluster-like agglomerates forming at the bottom, resulting in a clear dispersion (Figure S10). SEM observations, a 3D optical profiler, 3D-EEM, and flow cytometry confirmed the

spectrum of the M-Basswood exhibited a prominent new signal centered at 55.6 ppm, characteristic of a quaternary ammonium N-methyl carbon nucleus (C10),²⁷ originating from the cationization reaction between the epoxy group of CHPTAC and the hydroxyl groups of the basswood. This cationization reaction enables the introduction of the cationic functional group ($-(\text{CH}_2)_3\text{N}^+$) to the cellulose and hemicellulose backbone in the wood structure. The presence of the chemical grafting is also confirmed by XPS spectra, where the distinct C–N peak in the N 1s spectrum and the Cl⁻ peak in the Cl 2p spectrum^{28,29} appeared in the M-Basswood compared to the unmodified basswood, which was in good agreement with the FTIR and NMR results (Figure S6). As such, we evaluated the degree of substitution of CHPTAC on the wood substrate to be 0.169 ± 0.003 (Table S1) using the compositional cellulose as representative of basswood. Consequently, the decorated M-Basswood exhibited a positively charged surface (+24.3 mV), which is definitely the reverse of the natural basswood (–28.8 mV) (Figure 2F). The presence of such functional groups together with the 3D interconnected porous structure of the M-Basswood could potentially favor an efficient MNPs remediation from water systems.

As representatives of globally widespread MNPs in water ecosystems, polystyrene (PS) was selected to demonstrate the MNPs removal performance of M-Basswood. The biosafe and reliable M-Basswood with a positively charged surface was added to the negatively charged PS dispersions for MNPs remediation (Figure S7). Scanning electron microscopy (SEM) micrographs in Figure 2G showed that numerous spherical PS particles covered the entire outside surface and inside surfaces within the channels of M-Basswood. A closer observation further suggested the strong attachment of PS particles to M-Basswood (Figures 2H and 2I). Additionally, the 3D excitation-emission matrix (3D-EEM) fluorescence spectra of PS in water before and after treatment also indicated a noticeable decrease of PS particles in purified water (Figure 2J). Furthermore, measurement results from flow cytometry, a powerful tool for detecting the number of PS nanoparticles, demonstrated a substantial decrease in the number of PS particles after treatment with M-Basswood (Figure 2K). Overall, these results

excellent capture performance of M-Basswood (Figures S11–S14). The MNPs removal capacity and efficiency of M-Basswood were further quantified through fluorescence analysis (Figure S15). With an initial PS concentration of 1 mg/mL, M-Basswood achieved a capture capacity of 446.6 ± 0.4 – 491.8 ± 1.3 mg/g and a removal efficiency of 97.8%–99.8%, outperforming natural basswood by 5.5–45 times (Figure S16). By optimizing the capturing experiment parameters, for example, the dosage of M-Basswood, an improved capture capacity of 593.1 ± 0.02 mg/g and removal efficiency of 99.9% for PS-100 nm were achieved (Figure S17). Increasing the initial PS concentration to 2.0 mg/mL further enhanced the capture performance, reaching a maximum capacity of 926.7 ± 31.4 mg/g and an equilibrium removal efficiency of 97.6%–99.8% (Figure S18). M-Basswood also effectively captured irregular PS fragments and fibers (Figure S19), confirming its ability to handle different morphological MNPs.

Apart from MNPs' intrinsic features, the impact of environmental conditions on the removal effectiveness of M-Basswood was further investigated. Firstly, the capture performance of M-Basswood under different pH and salinity conditions using PS nanoparticles (100 nm, 1 mg/mL) was determined. The zeta potentials of PS dispersions remained stable between –51.1 and –39.7 mV across pH 3 to 11 (Figure S20). Different from other pH-dependent MNPs remediation studies,^{30–33} M-Basswood showed excellent capture performance across this wide pH range, with capacities of 456.4–462.6 mg/g and removal efficiencies of 99.5%–99.9%. Secondly, the impact of ionic strength was examined by using NaCl to simulate conditions from freshwater to salty water in the ocean. M-Basswood maintained high capture capacities (459.3–462.6 mg/g) and removal efficiencies (99.1%–99.8%) even at high salinity (Figure 3). Additionally, M-Basswood performed effectively under varying salt composition conditions, including NaNO₃, NaHCO₃, Na₂SO₄, KCl, and MgCl₂ (Figure S21). Thirdly, the influence of dissolved organic matter (DOM) having favorable attachment to MNPs was further explored. M-Basswood maintained high removal efficiencies (99.7%–99.8%) under different DOM conditions, such as humic acid and hydroquinone (Figure S22). These results demonstrated the stable and efficient MNPs

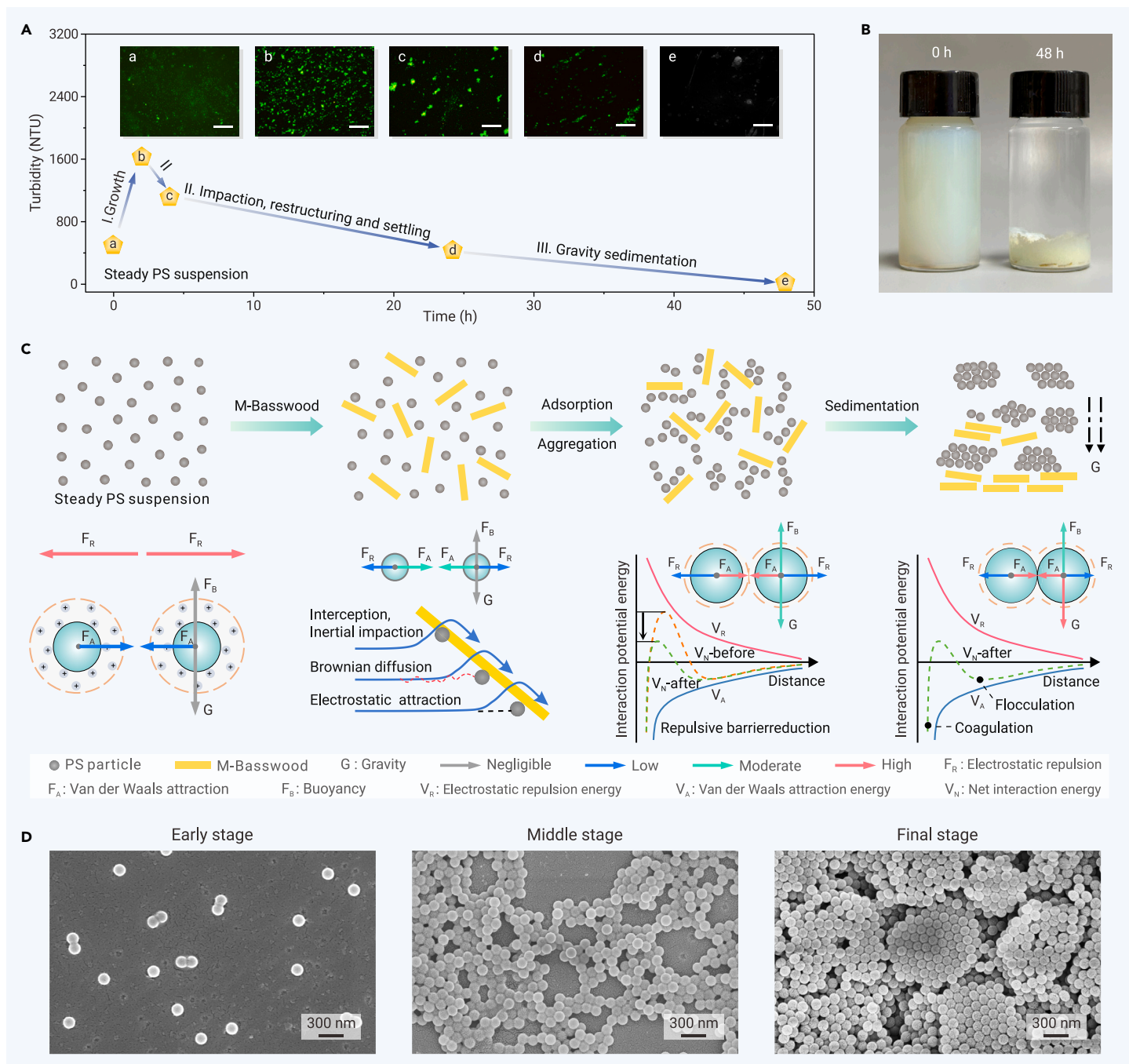


Figure 4. MNPs capture mechanisms of M-Basswood (A) Turbidity of PS dispersion over time. The insets show the fluorescence microscopy images of the upper dispersion collected at 0, 2, 4, 24, and 48 h, respectively. Scale bar: 100 μ m. (B) Photograph of PS dispersion before and after the M-Basswood treatment. (C) Illustration of multiscale interactions between M-Basswood and PS from macro to molecular views, as well as PS particle self-aggregations triggered by M-Basswood, with compressed electric double layer not shown for clarity. (D) SEM images of the early, middle, and final states of the M-Basswood and PS dispersion system.

capture performance of M-Basswood under various complex water conditions, providing great potential for MNPs remediation from practical wastewater.

Furthermore, to explore the capture effectiveness of M-Basswood upon different compositional MNPs, contaminated water systems containing various common waterborne MNPs, including polypropylene (PP), polyethylene (PE), polyvinyl chloride (PVC), and poly(methyl methacrylate) (PMMA) were tested. After treatment, all MNPs dispersions became clear, and SEM images showed captured MNPs on the surface and within the channels of the M-Basswood (Figures S10, S23 and S24). M-Basswood achieved capture capacities of 168.5 ± 2.4 mg/g for PE, 242.0 ± 1.5 mg/g for PP, 308.2 ± 2.2 mg/g for PVC, and 434.6 ± 3.9 mg/g for PMMA, demonstrating its broad-spectrum capture performance.

The universality of our proposed PCUS strategy to other types of biomass wastes was further investigated. Surface-modified straw (M-Straw; Figure S25) and bamboo waste (M-Bamboo; Figure S26) were prepared using the same method as M-Basswood. Impressively, both M-Straw and M-Bamboo delivered high PS removal efficiencies of 99.6–99.8%, suggesting the attractive universality of this PCUS strategy (Figures S25 and S26). This advantageous excellent removal performance toward different morphological, compositional, and dimensional MNPs, combined with high acid/basic tolerance and superior salt resistance, outperforming many other emerging adsorbents (Figure S27),^{34–38} positions our environmentally friendly woody biomass waste as a competitive candidate for sustainable water remediation applications.

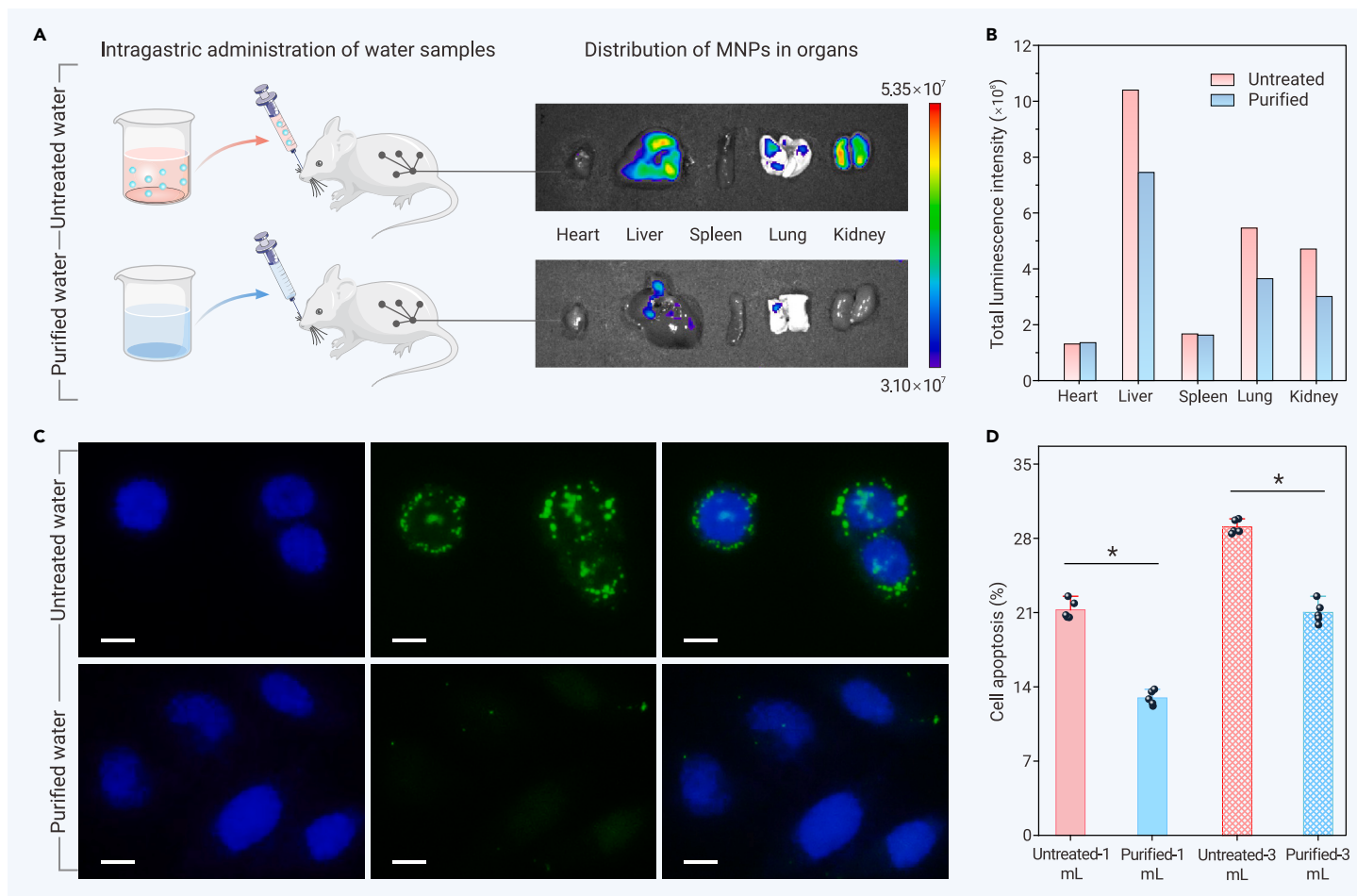


Figure 5. MNPs capture performance and potential effects on organs (A) Schematic illustration of the intragastric administration of two groups of mice (three in each group) with fluorescence-labeled PS-containing water and purified water by M-Basswood. *In vivo* imaging system (IVIS) revealing the concentration and distribution of PS nanoparticles in the mice organs, including heart, liver, spleen, lung, and kidney. (B) The fluorescence intensities of PS distributed in the mice organs intragastrically administered with PS-containing water and purified water, including the heart, liver, spleen, lung, and kidney. (C) Micrographs of MNPs immunofluorescence (green) in MIHA cells treated with co-culture for 24 h. Green fluorescence-labeled PS particles emitted fluorescence under the excitation/emission of 488/528 nm. DAPI (blue) was used to counterstain nuclei. Scale bar: 50 μm . (D) Flow cytometric analysis of MIHA cells apoptosis induced by different formulations under treatment or not by using Annexin V-FITC PI staining. PI, propidium iodide; FITC, fluorescein isothiocyanate. Data are mean \pm SD, * $p < 0.05$ by Student's two-tailed unpaired t test. $n = 5$ per group.

MNPs capture mechanisms of M-Basswood

To offer a deeper insight into the MNPs capture behavior of M-Basswood, we conducted an *in situ* investigation to observe the capturing process. Using a PS dispersion with 100 nm spherical nanoparticles as an example, we added positively charged M-Basswood to the dispersion until it became clear (Figure S28). A combination analysis of the fluorescence microscope images, hydrodynamic size distribution, and zeta potential of PS nanoparticles was performed to investigate their evolution (Figure S29). Upon adding M-Basswood, the PS dispersion became slightly turbid, and a noticeable cluster-like aggregation of PS nanoparticles occurred, with the particle size distribution broadening to the micron level (1–20 μm) within 2 h. Over time, PS micro-agglomerates dominated with a large particle size fraction of 88%, and as more aggregates settled, the dispersion became less cloudy. After 30 h, the macro-agglomerates (4–20 μm) had almost entirely settled, clearing the dispersion. Finally, all visible aggregates settled, leaving the dispersion transparent. This process was marked by changes in turbidity, which increased from 530 to 1,644 NTU (nephelometric turbidity units) within 2 h and then reduced to 7.99 NTU after 48 h (Figures 4A and 4B). Fluorescence microscope images also confirmed the aggregation and sedimentation of PS nanoparticles over time (inset of Figure 4A). By sharp contrast, adding natural basswood to the PS dispersion showed no hydrodynamic size change or visible PS particle aggregation, explaining its low capture efficiency (Figure S30). The zeta potential increased rapidly within 2 h and continued to rise to near zero after 24 h, reaching +22 mV after 48 h, revealing the physical-chemical driving forces involved in the PS capture process (Figure S29).

Figures 4C and 4D graphically and experimentally categorize the MNPs capture process by M-Basswood into three stages, respectively: (1) electrostatic sta-

bilization: in the early stage, well-dispersed colloidal PS nanoparticles accumulate the surface charge, forming an electrical double layer with a highly negative zeta potential (−38.0 mV). According to the classical Derjaguin, Landau, Verwey, and Overbeek theory,³⁹ repulsive forces maintain the stability of the colloidal PS system. (2) PS capturing and triggered self-aggregation: in the middle stage, PS particles are captured by positively charged M-Basswood via multiscale interactions, including physical trapping, hydrogen bonding, and strong electrostatic attraction (Figures 2G–2I, S31, and S32). As M-Basswood is added, the zeta potential changes, destabilizing the system and compressing the electrical double layer. The van der Waals attraction becomes dominant, causing PS particles to aggregate, forming micro- and macro-aggregates. (3) Sedimentation: in the final stage, larger clusters form through encounters between different clusters, leading to statistically self-similar, irregular aggregates (Figures 4D and S33). The larger the cluster size, the faster they settle. During settling, larger aggregates tend to gather and enwrap the smaller particles that are difficult to settle at the beginning, facilitating their removal from the water. These results demonstrate that M-Basswood effectively removes PS particles through multiscale interactions and triggered sedimentation, offering a facile and efficient method for MNPs remediation from water.

MNPs capture performance and potential effects on mice organs

After the capture of PS nanoparticles by M-Basswood, the fluorescence intensity of fluorescence-labeled PS was reduced by ~99.8% in the water, indicating the excellent removal of PS (Figure S34). Considering MNPs with a smaller size have a higher probability of being absorbed and present in the human bloodstream, the PS-containing water and the purified water before and after

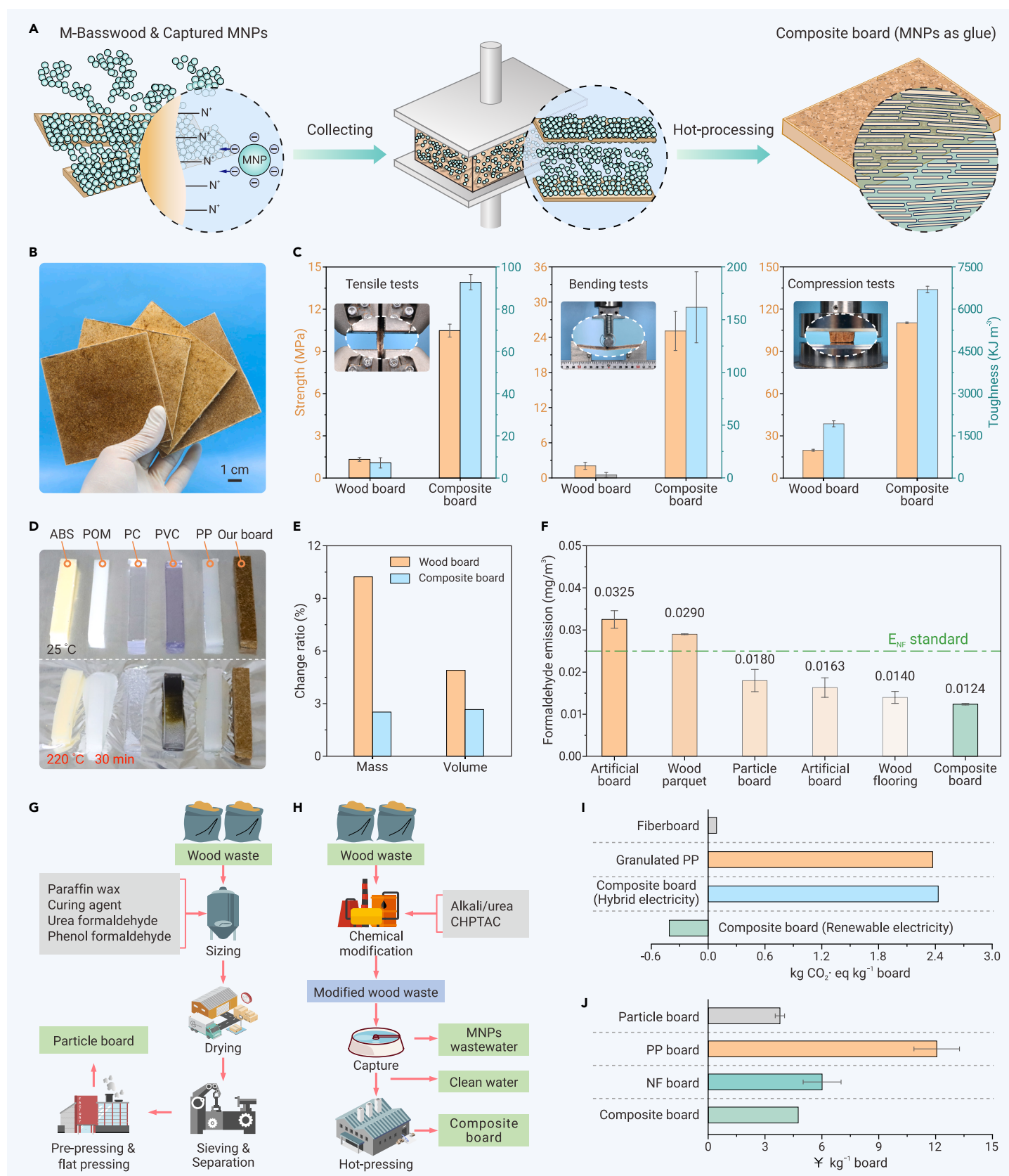


Figure 6. Sustainable MNPs utilization and storage with environmental and economic benefits (A) Illustration of MNPs-captured M-Basswood followed by hot pressing to produce a final composite board, in which the captured MNPs served as a glue to enhance the processability and comprehensive performance of the composite board. (B) Photograph of the composite board. (C) Mechanical performance of the natural wood board with no MNPs and composite board with captured MNPs ($n = 3$, error bar represents the standard error of the mean). (D) Thermal stability of the composite board. (E) Hygroscopic behavior of wood board and composite board at a high air relative humidity of 97%. (F) Formaldehyde emissions of the composite board compared to other advanced artificial boards and limited value according to Chinese National Standard GB/T 39600-2021 ($n = 3$, error bar represents the standard error of the mean). (G and H) Comparison of current manufacturing routes of commercial particle board (G) to our composite board based on PCUS strategy (H). (I) Comparison of greenhouse gas (GHG) emissions of our composite board with current routes to fiberboard and granulated PP according to life cycle assessment (LCA). (J) Comparison of the economic cost of our composite board with current routes to commercial particle board, PP board, and no-formaldehyde (NF) board via TEA.

M-Basswood treatment were intragastrically administered to two groups of mice (three in each group) every 24 h to investigate whether and where the uptake and accumulation of MNPs occurred in the mice (Figures 5A and S35). After 1 week of intragastric administration, the fluorescence intensity distributed in the organs of mice from the two groups was determined using an *in vivo* imaging system (IVIS). The IVIS spectra indicated lower fluorescence intensities of the organs in mice administered with purified water compared to the ones administered with the untreated PS dispersion, verifying the efficient removal of PS nanoparticles by M-Basswood and thus limited accumulation in organs (Figures 5A and 5B). Additionally, to reveal the potential impacts of the accumulated nanoplastics on the main organs of mice, the H&E-stained liver, lung, and kidney tissues of the two groups of mice were observed and photographed for analysis (Figure S36). Compared to the purified-water-administered mice, more visible histopathological damage was found in the three organs of PS-containing-water-administered mice after a week of gavage, indicating a strong correlation to the uptake and accumulation of PS in the organs and thus toxicity to the mice. More intuitively, it was observed that a large number of PS nanoplastics were taken up and accumulated in immortalized human hepatocytes (MIHA cells) exposed to PS-contaminated water (Figures 5C and 5D). By sharp contrast, no significant fluorescence signal was observed in the cells exposed to purified water. These results demonstrated that the treatment of MNPs-containing water by M-Basswood profoundly mitigates the risks of ingestion and accumulation of MNPs in aquatic organisms, leading to substantially reduced toxicity and improved biosafety to the water ecosystem.

Sustainable MNP utilization and storage with environmental and economic benefits

Instead of solely using MNPs for water remediation purposes, we offer full-chain, biomass-waste-assisted PCUS solutions, seamlessly gathering all elements of the equation to deliver value from start to finish. Figure 6A graphically illustrates the production process of composite (wood-plastic) boards via an industrially mature technique of hot pressing, a process that enables “locking in” MNPs for much longer and more productive use. Specifically, the recycled MNPs served as a functional adhesive for the build-up of a high-performance composite material (Figures 6A and 6B). Hot pressing leads to the complete collapse of wood lumina and cell walls of M-Basswood, creating a unique “MNPs glued wood fibers” microstructure. The SEM images in Figure S37 reveal tightly intertwined and densely packed wood cell walls. Leveraging the high mechanical properties of wood and the enhanced adhesion of M-Basswood by the captured MNPs, the composite board achieved a tensile strength of 10.5 MPa, a flexural strength of 25.1 MPa, and a compressive strength of 110.3 MPa—8.1, 12.0, and 5.6 times higher than pure wood board without recycled MNPs, respectively (Figure 6C). The composite board exhibited no visible thermal shrinkage or structural collapse even after being heated at 220 °C for 30 min, whereas the other five commercial plastic boards including acrylonitrile butadiene styrene (ABS), polyoxymethylene (POM), polycarbonate (PC), PVC, and PP showed severe dimensional deformation and softening (Figures 6D and S38). Attractively, the MNPs-adhesive composite board also demonstrated outstanding thermal and mechanical properties (Figures S39 and S40), moisture resistance (Figure 6E), and weathering stability when exposed to a highly humid environment (Figure S41) and ultraviolet irradiation conditions for 2 weeks (Figure S42), indicating its potential for practical application. Of note, while short-term tests are promising, evaluating long-term weathering stability remains challenging due to complex conditions, necessitating further studies. Additionally, our composite board’s formaldehyde emission of 0.0124 mg/m³, tested per Chinese National Standard GB/T 41649-2022, is lower than the 0.025 mg/m³ limit for no-formaldehyde wood-based panels according to Chinese National Standard GB/T 39600-2021 and superior to other commercial artificial boards (Figure 6F).^{40–44} This formaldehyde-free composite board with captured MNPs as an adhesive represents a sustainable alternative to traditional wood-based panels using phenol- and urea-formaldehyde adhesives.

Incorporating MNPs into value-added products well aligns with the circular economy by introducing potentially hazardous waste back into the economic cycle. To assess the environmental and economic sustainability of our PCUS process, we performed life cycle assessment (LCA) and techno-economic analysis (TEA) studies, using the current particle board as a control (Figures 6G and 6H). The greenhouse gas emissions over a 100 year time horizon for our composite

board were evaluated regarding the global warming potential (GWP) impact category (ReCiPe 2016 Midpoint H methodology, Tables S2 and S3). Our composite board has a cradle-to-gate GWP value of 3.71 kg CO₂ equiv kg⁻¹ when using an electricity production mix from China (Figures 6I and S43). Considering the carbon sequestration ability of dry wood (1.72 kg CO₂/kg) and the credits from plastic waste landfill diversion (0.254 kg CO₂ equiv kg⁻¹),⁴⁵ the net GWP is reduced to 2.43 kg CO₂ equiv kg⁻¹. As shown in Figures 6I and S44, this value is comparable to granulated PP (2.37 kg CO₂ equiv kg⁻¹) and lower than those of other fossil-based materials such as PC (5.30 kg CO₂ equiv kg⁻¹) and glass fiber reinforced polyester (3.77 kg CO₂ equiv kg⁻¹). However, it is higher than the carbon footprint of fiberboard production (0.08 kg CO₂ equiv kg⁻¹), which benefits from a non-fossil carbon dioxide resource correction. As such, a careful look at the process contribution could shed light on the larger impacts obtained. Figure S45 indicates that electricity is the primary contributor to the composite board’s GWP, accounting for 87.60% of total emissions (3.25 kg CO₂ equiv kg⁻¹), due to China’s coal-dominated energy mix (>55%). A renewable energy scenario reduces the carbon footprint to -0.41 kg CO₂ equiv kg⁻¹, surpassing commercial fiberboard in various environmental metrics (Table S4). Replacing conventional melamine-urea-formaldehyde adhesives (GWP 2.82 kg CO₂ equiv kg⁻¹) with MNPs could make materials carbon-negative, demonstrating the potential for CO₂ removal and decarbonizing materials.^{46–48} Additionally, PP MNPs enhance other impact categories such as fossil resource scarcity and water consumption as well (Figure S46). Despite low-scale fabrication and the low technology readiness level possibly overestimating environmental impacts, our study provides encouraging data for expanding low-carbon materials production from biomass and plastic wastes.

As a key emission reduction technology, the technical economics of the PCUS strategy is also crucial. Therefore, we conducted a TEA to investigate the economic cost of producing our composite board (Figure 6J). The production cost of our composite board is 4.7 ¥/kg considering the Wuhan (China)-based plant (Table S5), which is lower than conventional petroleum-derived materials like high-density PE (8.4 ¥/kg) or PP (12.1 ¥/kg)⁴⁹ and no-formaldehyde boards (6.0 ¥/kg). It is also comparable to particle board (3.8 ¥/kg) and formaldehyde-free boards (5.0–7.0 ¥/kg). These findings show that the PCUS strategy is environmentally sustainable, reliable, and economically feasible, offering a new pathway for MNPs-derived products and playing a significant role in reducing microplastics pollution while mitigating economic impact. However, several concerns about scalability must be addressed for real-world applications, including the trade-offs among stable product performance, environmental sustainability, and cost effectiveness and the role of government regulations and collaborative innovations in shaping the PCUS market.

CONCLUSION

In summary, we demonstrated an environmentally and economically sustainable biomass waste-assisted PCUS concept as a multifaceted approach to manage MNPs pollution, promising to make up the vast majority of mitigation of net-zero plans in the longer term. M-Basswood, as the capturing material, exhibited excellent capture performance to a broad spectrum of MNPs under different environmental conditions, suggesting its great potential for MNPs removal from practical wastewater. This excellent capture performance was driven by the multiscale interactions between M-Basswood and MNPs (e.g., physical trapping, hydrogen bonding, π - π stacking, and strong electrostatic attraction), as well as triggered cluster-like self-aggregation sedimentation of MNPs. As a result of the effective removal of MNPs from water, the *in vivo* bio-distribution of MNPs in the organs of mice demonstrated low risks of ingestion and accumulation of MNPs in aquatic organisms and low toxicity to the water ecosystem. In addition to water remediation, the captured MNPs, together with the woody biomass waste, were directly processed into composite (wood-plastic) boards via an industrially mature technique of hot pressing for further utilization and storage. This composite board demonstrated excellent mechanical properties, outstanding thermal stability, good moisture resistance, and extremely low formaldehyde emission. More importantly, LCA and TEA results demonstrated the low environmental impacts and high economic feasibility of the integrated PCUS approach. The reliable, environmentally friendly, and cost-effective PCUS strategy enables MNPs remediation from water and value-added productive reuse, which is expected to advance the global goal of safe and environmentally sound management of plastics.

MATERIALS AND METHODS

Materials

Wood waste with 30 mesh sieve size was provided by Guangzhou Zhicheng Wood Industry (Guangzhou, China). MNPs with different sizes, shapes, and chemical compositions were used in this work. Fluorescence-labeled PS dispersions (spheres and fragments, 30 nm, 100 nm, 500 nm, 1 μ m, 5 μ m, and 10 μ m, 2.5 wt%) with an excitation/emission wavelength at 488/528 nm, and PMMA particles (spheres, 100 nm, 2.5 wt%) were purchased from Jiangsu Zhichuan Technology Co., Ltd (Jiangsu, China). PS fibers dispersions were purchased from Kaixuan Plastic Technology Co., Ltd (Guangdong, China). PVC particles (spheres, 1 μ m) were purchased from Tesulang Chemical Materials (Dongguan, China). PP particles (spheres, 500 nm) and PE particles (spheres, 500 nm) were provided by Guangdong Wengjiang Chemical Reagent (Guangdong, China). The PVC, PP, and PE MNPs were dispersed in deionized (DI) water and Tween 80 with ultrasonic assistance. The commercial plastic boards including ABS copolymers, polyacetal (POM), PC, PVC, and PP were provided by Suzhou Dichuang Plastic Industry (Suzhou, China). All other chemicals and reagents, CHPTAC (60 wt %), sodium hydroxide (NaOH, $\geq 96\%$), and urea ($\geq 99\%$), were purchased from Sino-pharm Chemical Reagent (Shanghai, China).

Surface functionalization of wood waste

Wood waste was functionalized with CHPTAC following a procedure established in our group. Briefly, basswood sawdust (1 g) was added into a pre-cooled ($-12\text{ }^{\circ}\text{C}$) aqueous solution (7 wt % NaOH, 12 wt % urea, and 81 wt % H_2O). Then, the dispersion was transferred into a vacuum chamber, followed by a 30 min vacuum treatment under 20 Pa to ensure the mixed solution throughout flowed into the channels, which was repeated three times. Thereafter, the CHPTAC (4 g) was added dropwise into the dispersion under magnetic stirring for 10 h at $65\text{ }^{\circ}\text{C}$. The collected M-Basswood was diluted with DI water to remove the residual chemicals and, finally, dried at $80\text{ }^{\circ}\text{C}$ overnight.

REFERENCES

- Stegmann, P., Daioglou, V., Londo, M., et al. (2022). Plastic futures and their CO₂ emissions. *Nature* **612**: 272–276. <https://doi.org/10.1038/s41586-022-05422-5>.
- MacLeod, M., Arp, H.P.H., Tekman, M.B., et al. (2021). The global threat from plastic pollution. *Science* **373**(6550): 61–65. <https://doi.org/10.1126/science.abg5433>.
- Xia, Q., Chen, C., Yai, Y., et al. (2021). A strong, biodegradable and recyclable lignocellulosic bioplastic. *Nat. Sustain.* **4**: 627–635. <https://doi.org/10.1038/s41893-021-00702-w>.
- Lau, W.W.Y., Shiran, Y., Bailey, R.M., et al. (2020). Evaluating scenarios toward zero plastic pollution. *Science* **369**(6510): 1455–1461. <https://doi.org/10.1126/science.aba9475>.
- Jambeck, J.R., Geyer, R., Wilcox, C., et al. (2015). Marine pollution. Plastic waste inputs from land into the ocean. *Science* **347**(6223): 768–771. <https://doi.org/10.1126/science.1260352>.
- Li, C., Gillings, M.R., Zhang, C., et al. (2024). Ecology and risks of the global plastisphere as a newly expanding microbial habitat. *Innovation* **5**(1): 100543. <https://doi.org/10.1016/j.xinn.2023.100543>.
- Santos, R.G., Machovsky-Capuska, G.E., Andrades, R., et al. (2021). Plastic ingestion as an evolutionary trap: toward a holistic understanding. *Science* **373**(6550): 56–60.
- Stubbins, A., Law, K.L., Muñoz, S.E., et al. (2021). Plastics in the Earth system. *Science* **373**(6550): 51–55. <https://doi.org/10.1126/science.abb0354>.
- Mennekes, D., and Nowack, B. (2023). Predicting microplastic masses in river networks with high spatial resolution at country level. *Nat. Water* **1**: 523–533. <https://doi.org/10.1038/s44221-023-00090-9>.
- Tessnow-von Wysocki, I., Wang, M., Morales-Caselles, C., et al. (2023). Plastics treaty text must center ecosystems. *Science* **382**(6670): 525–526. <https://doi.org/10.1126/science.adl3202>.
- (2023). Zero draft text of the international legally binding instrument on plastic pollution, including in the marine environment. United Nations Environment Programme. <https://wedocs.unep.org/handle/20.500.11822/43239>.
- Fankhauser, S., Smith, S.M., Allen, M., et al. (2022). The meaning of net zero and how to get it right. *Nat. Clim. Chang.* **12**: 15–21. <https://doi.org/10.1038/s41558-021-01245-w>.
- Yang, Q., Zhou, H., Bartocci, P., et al. (2021). Prospective contributions of biomass pyrolysis to China's 2050 carbon reduction and renewable energy goals. *Nat. Commun.* **12**: 1698. <https://doi.org/10.1038/s41467-021-21868-z>.
- Afful-Dadzie, A. (2021). Global 100% energy transition by 2050: A fiction in developing economies? *Joule* **5**(7): 1641–1643. <https://doi.org/10.1016/j.joule.2021.06.024>.
- Markewitz, P., Kuckshinrichs, W., Leitner, W., et al. (2012). Worldwide innovations in the development of carbon capture technologies and the utilization of CO₂. *Energy Environ. Sci.* **5**(6): 7281–7305. <https://doi.org/10.1039/C2EE03403D>.
- Wang, F., Harindintwali, J.D., Yuan, Z., et al. (2021). Technologies and perspectives for achieving carbon neutrality. *Innovation* **2**(4): 100180. <https://doi.org/10.1016/j.xinn.2021.100180>.
- Langie, K.M.G., Tak, K., Kim, C., et al. (2022). Toward economical application of carbon capture and utilization technology with near-zero carbon emission. *Nat. Commun.* **13**: 7482. <https://doi.org/10.1038/s41467-022-35239-9>.
- Mertens, J., Breyer, C., Arning, K., et al. (2023). Carbon capture and utilization: more than hiding CO₂ for some time. *Joule* **7**(3): 442–449. <https://doi.org/10.1016/j.joule.2023.01.005>.
- (2019). Zion Market Research: Carbon Capture, Utilization, and Storage (CCUS) Technologies Market Size Report, Industry Share, Analysis, Growth, 2030: Zion Market Research (Globe Newswire). <https://www.zionmarketresearch.com/report/carbon-capture-utilization-and-storage-ccus-technologies-market>.
- (2018). Facts and figures on materials, wastes and recycling (National Overview). <https://www.epa.gov/facts-and-figures-about-materials-waste-and-recycling/national-zverview-facts-and-figures-materials>.
- Dong, X., Gan, W., Shang, Y., et al. (2022). Low-value wood for sustainable high-performance structural materials. *Nat. Sustain.* **5**: 628–635. <https://doi.org/10.1038/s41893-022-00887-8>.
- Wang, Y., Wang, M., Wang, Q., et al. (2023). Flowthrough capture of microplastics through polyphenol-mediated interfacial interactions on wood sawdust. *Adv. Mater.* **35**: 2301531. <https://doi.org/10.1002/adma.202301531>.
- Wang, B., Wang, J., Hu, Z., et al. (2024). Harnessing renewable lignocellulosic potential for sustainable wastewater purification. *Research* **7**: 0347. <https://doi.org/10.34133/research.0347>.
- Wang, Z., Xu, C., Qi, L., et al. (2024). Chemical modification of polysaccharides for sustainable bioplastics. *Trends Chem.* **6**(6): 314–331. <https://doi.org/10.1016/j.trechm.2024.04.009>.
- Phillips, D.L., Xing, J., Liu, H., et al. (1999). Raman spectroscopic determination of the degree of cationic modification in waxy maize starches. *Anal. Lett.* **32**(15): 3049–3058. <https://doi.org/10.1080/00032719908543026>.
- Chen, G., Li, T., Chen, C., et al. (2019). A highly conductive cationic wood membrane. *Adv. Funct. Mater.* **29**: 1902772. <https://doi.org/10.1002/adfm.201902772>.
- Song, Y., Sun, Y., Zhang, X., et al. (2008). Homogeneous quaternization of cellulose in NaOH/urea aqueous solutions as gene carriers. *Biomacromolecules* **9**(8): 2259–2264. <https://doi.org/10.1021/bm800429a>.
- Tsimpouki, L., Papapetros, K., Anastasopoulos, C., et al. (2023). Water-soluble quaternized copolymers as eco-friendly cationic modifiers of cotton fabrics for salt-free reactive dyeing applications. *Cellulose* **30**: 6031–6050. <https://doi.org/10.1007/s10570-023-05220-w>.
- Wang, L., Du, Y., Zhu, Q., et al. (2023). Regulating the alkyl chain length of quaternary ammonium salt to enhance the inkjet printing performance on cationic cotton fabric with reactive dye ink. *ACS Appl. Mater. Interfaces* **15**(15): 19750–19760. <https://doi.org/10.1021/acami.3c02304>.
- Xiong, Y., Zhao, J., Li, L., et al. (2020). Interfacial interaction between micro/nanoplastics and typical PPCPs and nanoplastics removal via electrosorption from an aqueous solution. *Water Res.* **184**: 116100. <https://doi.org/10.1016/j.watres.2020.116100>.
- Sun, C., Wang, Z., Zheng, H., et al. (2021). Biodegradable and re-usable sponge materials made from chitin for efficient removal of microplastics. *J. Hazard Mater.* **420**: 126599. <https://doi.org/10.1016/j.jhazmat.2021.126599>.
- Wang, Z., Sun, C., Li, F., et al. (2021). Fatigue resistance, re-usable and biodegradable sponge materials from plant protein with rapid water adsorption capacity for microplastics removal. *Chem. Eng. J.* **415**: 129006. <https://doi.org/10.1016/j.cej.2021.129006>.
- Fu, J., Liu, N., Peng, Y., et al. (2023). An ultra-light sustainable sponge for elimination of microplastics and nanoplastics. *J. Hazard Mater.* **456**: 131685. <https://doi.org/10.1016/j.jhazmat.2023.131685>.
- Yen, P.L., Hsu, C.H., Huang, M.L., et al. (2022). Removal of nano-sized polystyrene plastic from aqueous solutions using untreated coffee grounds. *Chemosphere* **286**: 131863. <https://doi.org/10.1016/j.chemosphere.2021.131863>.
- Wang, J., Sun, C., Huang, Q.X., et al. (2021). Adsorption and thermal degradation of microplastics from aqueous solutions by Mg/Zn modified magnetic biochars. *J. Hazard Mater.* **419**: 126486. <https://doi.org/10.1016/j.jhazmat.2021.126486>.
- Zheng, B., Li, B., Wan, H., et al. (2022). Coral-inspired environmental durability aerogels for micron-size plastic particles removal in the aquatic environment. *J. Hazard Mater.* **431**: 128611. <https://doi.org/10.1016/j.jhazmat.2022.128611>.
- Urso, M., Ussia, M., Novotný, F., et al. (2022). Trapping and detecting nanoplastics by MXene-derived oxide microrobots. *Nat. Commun.* **13**: 3573. <https://doi.org/10.1038/s41467-022-31161-2>.
- Shi, X., Zhang, X., Gao, W., et al. (2022). Removal of microplastics from water by magnetic nano-Fe₃O₄. *Sci. Total Environ.* **802**: 149838. <https://doi.org/10.1016/j.scitotenv.2021.149838>.
- Derjaguin, B., and Landau, L. (1993). Theory of the stability of strongly charged lyophobic sols and of the adhesion of strongly charged particles in solutions of electrolytes. *Prog. Surf. Sci.* **43**: 30–59. [https://doi.org/10.1016/0079-6816\(93\)90013-L](https://doi.org/10.1016/0079-6816(93)90013-L).
- Han, Y. A formaldehyde treatment agent for man-made boards and its preparation method and application. Patent CN114517040A.
- Xu, M., Fang, C., Wu, Z. Low-formaldehyde and high-quality solid wood composite floor and its processing technology. Patent CN112917618A.
- Liu, M., Wu, Z., Cai, Q., et al. An environmentally friendly homogeneous super-strong particle-board and its preparation method. Patent CN113119267A.
- Du, G., Deng, S., Yang, L., et al. ENF grade wood-based panel adhesive and its preparation method. Patent CN114891468A.
- Sun, W. A Stone Wood Floor and its Preparation Method. Patent CN116717048A.
- Eriksson, O., and Finnveden, G. (2009). Plastic waste as a fuel-CO₂-neutral or not? *Energy Environ. Sci.* **2**: 907–914. <https://doi.org/10.1039/B908135F>.

46. Daehn, K., Basuhi, R., Gregory, J., et al. (2021). Innovations to decarbonize materials industries. *Nat. Rev. Mater.* **7**: 275–294. <https://doi.org/10.1038/s41578-021-00376-y>.
47. Ma, D. (2023). Transforming end-of-life plastics for a better world. *Nat. Sustain.* **6**: 1142–1143. <https://doi.org/10.1038/s41893-023-01224-3>.
48. Schneider, F., Parsons, S., Clift, S., et al. (2023). Life cycle assessment (LCA) on waste management options for derelict fishing gear. *Int. J. Life Cycle Assess.* **28**: 274–290. <https://doi.org/10.1007/s11367-022-02132-y>.
49. (2023). Weekly commodity price report, prices for this week 24/2023 (PlasticPortal). <https://www.plasticportal.eu/en/cenove-report/>.

ACKNOWLEDGMENTS

C.C. thanks the National Natural Science Foundation of China (grant no. 52273091), Knowledge Innovation Program of Wuhan-Basi Research (grant no. 2023020201010072), and the Fundamental Research Funds for the Central Universities (grant no. 691000003) for the financial support. E.L. thanks the University of the Basque Country (Convocatoria de ayudas a grupos de investigación, GIU21/010) for the financial support. We thank the Test Center and Core Facility of Wuhan University for assistance with material characterizations.

AUTHOR CONTRIBUTIONS

C.C. conceived the concept and supervised the work. L.C. and T.B. carried out most experiments. E.L. contributed to the LCA and TEA. A.L. contributed to the animal experiments and analyzed the results. L.Q. contributed to the graphical illustrations. Y.M. and Z.L. assisted in the synthesis of samples. J.H. contributed to sample characterizations. C.C., H.D., and L.C. analyzed the data and co-wrote the manuscript. C.C., H.D., L.C., and L.Y. revised the manuscript. All authors commented on the submitted version of the manuscript.

DECLARATION OF INTERESTS

The authors declare no competing interests.

SUPPLEMENTAL INFORMATION

It can be found online at <https://doi.org/10.1016/j.xinn.2024.100655>.

LEAD CONTACT WEBSITE

<https://biomass.whu.edu.cn/index.htm>